Effective antireflection and surface passivation of silicon using a SiO_2/a-TiO_x film stack

Ruy S. Bonilla, Kristopher O. Davis, Eric J. Schneller, Winston V. Schoenfeld and Peter R. Wilshaw

***Abstract*—This article reports an effective and industrially relevant passivation and anti-reflection film stack featuring a 10 nm silicon dioxide (SiO_2) film followed by a ≈65 nm amorphous titanium oxide (a-TiO_x) film. This film stack has equivalent optical performance to a single-layer silicon nitride (SiN_x) anti-reflection coating (ARC) for unencapsulated cells, and slightly better performance for encapsulated cells (≈0.2 mA·cm^{-2} increase). The field effect passivation properties of the SiO_2/a-TiO_x film stack have been modified extrinsically after the film deposition to demonstrate surface recombination velocities below 1.2 cm/s in a 1 Ω·cm n-type silicon wafer. Finally, the TiO_x films have been deposited using an in-line atmospheric pressure chemical vapor deposition (APCVD) system at temperatures below 350^{o}C, thus demonstrating this film stack offers both better passivation and optical performance, as well as a potentially lower manufacturing cost compared to SiN_x, due to the use of APCVD rather than plasma-enhanced chemical vapor deposition. Simulations indicate further gains in terms of optical performance (≈0.3 mA·cm^{-2} increase compared to SiN_x – encapsulated case) may be possible using a double-layer ARC featuring a polycrystalline TiO_x (pc-TiO_x) film followed by an aluminum oxide (AlO_x). However, potential contamination from the APCVD may pose a risk to maintaining high bulk carrier lifetimes.**

***Index Terms*— Silicon solar cells, antireflection dielectric coating, surface passivation, field effect**

I. Introduction

SILICON photovoltaic devices have been the workhorse of solar electricity generation in the past two decades. During this time, several advances in the manufacturing processes of silicon cells have been successfully transferred from laboratories to large scale production lines. These include better contact formation and metallization technologies, cleaner and higher performance silicon material, and effective dielectric coatings that act as passivation and antireflection layers when placed on the surface of a solar cell. Such dielectric coatings are fundamental to the high performance of solar cells and as such have been much researched. Titanium oxide (TiO_x) was the antireflection coating of choice when commercial production of silicon solar cells increased in the 1980-90's [1]–[3]. TiO_x was used since it showed optimal optical properties to act as an antireflection coating between a silicon surface and an Ethylene Vinyl Acetate (EVA) encapsulant film used when packing cells into modules [4]. Deposition of TiO_x was performed using either chemical [5] or physical vapor techniques [4], and its use extended beyond that of the solar industry, most prominently in glass manufacturing as a protection coating deposited with ultra-high throughput techniques [6], [7]. Despite its ideal optical properties, TiO_x was quickly replaced by hydrogenated silicon nitride (SiN_x) since the evolution of silicon solar cells required appropriate passivation of the cells' front surface, and this could not be accomplished using TiO_x [8]. SiN_x, typically deposited using plasma enhanced chemical vapor deposition (PECVD), has been extensively studied to achieve films that provide very effective surface passivation to both n- and p-type silicon surfaces [9]. The passivation quality of these nitride films originates both in the efficient saturation of Si dangling bonds at the interface [10], and a concentration of permanent charge that provides field effect passivation by modifying the concentration of carriers at the surface [11]. Currently, industrial scale PECVD deposition of SiN_x is widely used as the preferred method to provide passivation and antireflection to the cell's front surface. PECVD silicon nitride, however, has a number of disadvantages. Firstly, it requires a vacuum for the film deposition process, secondly, it typically presents a concentration of positive charge thus being less efficient at passivating p-type surfaces, thirdly, it has maximum refractive index of ~2.1 for a Si rich film [12], [13], thus being a less ideal ARC between silicon and EVA, and lastly, the precision and sensitivity of the PECVD deposition process leads to a trade-off between the optical and passivation properties that can be achieved in a single film.

In recent years, double layer antireflection coatings (DLARC) have been used in high-efficiency cell architectures where improved chemical passivation is desired and normally achieved by using a thermally grown silicon dioxide (SiO_2) interlayer. This interlayer largely decouples the requirement for a single, for instance SiN_x, layer to provide both effective passivation and antireflection. When used as the second layer in a DLARC, SiN_x still shows substantially better optical

This work was supported by the EPSRC (UK) Postdoctoral Research Fellowship, EP/M022196/1 and grant EP/M024911/1.

R. S. Bonilla and P. R. Wilshaw are with the Department of Materials, University of Oxford, Parks Rd, Oxford, OX1 3PH, UK. (e-mails: sebastian.bonilla@materials.ox.ac.uk, peter.wilshaw@materials.ox.ac.uk).

K. O. Davis and E. J. Schneller are with the Florida Solar Energy Center and the Department of Materials Science and Engineering, University of Central Florida, Orlando, FL 32816 USA (e-mails: kdavis@fsec.ucf.edu, eschneller@fsec.ucf.edu).

W. V. Schoenfeld is with the College of Optics and Photonics and the Department of Electrical and Computer Engineering, University of Central Florida, Orlando, FL 32826 USA (e-mail: winston@fsec.ucf.edu)

performance than other dielectrics like aluminum oxide (AlO_x) [14], silicon oxide (SiO_x) [15] and silicon carbide (SiC_x) [16], while the additional passivation achieved by fixed charge and by the hydrogenation process during PECVD deposition [17] makes it preferable to TiO_x. In recent years, however, Thomson and McIntosh demonstrated reasonable silicon surface passivation using low temperature atmospheric pressure chemical vapor deposition (APCVD) of TiO_x [18]. In their work they demonstrated moderate levels of passivation when TiO_x coated Si was subjected to anneal and light soaking steps. In addition to this, other recent reports have shown that the passivation quality of many dielectric coatings can be strongly modified by using processing steps applied after the film has been deposited, here referred to as extrinsic passivation. These include the well-known forming gas anneal that hydrogenates the dielectric/silicon interface [19], the post-deposition activation anneal that produces large concentrations of, for example, negative charge in AlO_x films [20], and the incorporation of charged ions into dielectric coatings that increase the field effect passivation in the film [21]. If these electrical properties are combined with the ability to tailor the optical properties in TiO_x films [22], a very effective film stack is possible.

In this work we report an extremely effective passivation and ARC consisting of thermal SiO_2 and APCVD TiO_x, which is directly applicable to the industrial manufacture of high efficiency silicon solar cells. The films' optical properties were tailored in the APCVD deposition process while passivation properties were modified extrinsically (after film growth/deposition) by introducing corona ions into the dielectric stack. These ions modify the surface charge carrier concentration via the field effect to reduce the surface recombination rate. Here, we first report the experimental methodology used to produce silicon specimens with this DLARC, we then show the electrical and optical properties achieved in the dielectric system as a function of the different processing steps, and highlight the impact that these methods can have in the progress of silicon photovoltaic technology.

II. Sample Preparation and Characterization

The optical and passivation properties of the SiO_2/TiO_x dielectric system were studied using planar, 1 Ωcm, <100>, *n*-type float zone silicon. Wafers were Radio Corporation of America (RCA) cleaned prior to oxidation in a Centrotherm tube furnace, in a dry environment at either 850 °C to produce 10 nm SiO_2, or 1050 °C to produce 100 nm SiO_2. This was performed at Fraunhofer ISE. A subset of industrial-scale wafers (156 mm x 156 mm) were texturized with random pyramids using an IPA/KOH anisotropic etch prior to the RCA clean. After oxidation, wafers were deposited on both surfaces with an amorphous TiO_x film using an in-line industrial SierraTherm 5500 APCVD system (now SCHMID), at a set temperature of 350 °C, with an actual deposition temperature of 250±10 °C. Deposition took place by placing the silicon wafers on a continuously moving belt which horizontally transported the wafers under the APCVD deposition chamber. Tetraisopropyl titanate (TPT) and H_2O were used as precursors in a ratio ≈1.4 H_2O:TPT, to obtain the desired refractive index. In addition to the low temperature a-TiO_x, an APCVD double layer of 40 nm polycrystalline (pc) TiO_x / 70 nm AlO_x was also deposited at a temperature of 570 °C as detailed in reference [22]. As a comparison for the reflectance measurements, a ≈70 nm PECVD SiN_x film was also deposited onto textured wafers using a Roth & Rau SINA PECVD system. Silane and ammonia were used as precursor gases, and the gas-flux ratio optimized to achieve a refractive index of ~2.1 at 630 nm.

Electrical characterization of the dielectric films was performed using capacitance- and conductance-voltage (CGV) measurements with a Keysight E4980A LCR meter for the frequency regime 20 Hz-2 MHz. The electrical properties of the APCVD TiO_x film were independently studied by depositing it directly on a RCA cleaned bare n-type Cz Si substrate, 10 Ωcm, without a SiO_2 film. Metal-insulator-semiconductor (MIS) structures were formed on single TiO_x, single SiO_2, and double SiO_2/ TiO_x layer systems by depositing ≈50 nm thickness of aluminum using thermal evaporation through a shadow mask to form front contacts, ≈1 mm diameter. The exact contact area (A) of the Al contact was measured using calibrated microscope images, and this value used for the processing of CGV data. Back contacts were formed using a Gallium-Indium eutectic. The flat-band voltage V_{fb} was found by correcting the measured gate voltage V_g to account for the stretching produced by interface states D_{it} thus producing a V_{g0}. The measured high frequency capacitance C_{HF} vs. V_{g0} curve was translated on the voltage axis to find the V_{fb} that produced the best fit between the measured and the theoretical relations. V_{fb} was used to calculate the dielectric fixed charge Q_f as detailed in [23]. The insulator capacitance C_i was determined in the accumulation regime using the McNutt-Sah method [24] with the extension in [25], and used to calculate the effective oxide thickness using $EOT = \varepsilon_0 K_{SiO_2} Area/C_i$. An expansion of these methods is found in [26].

A Sinton WCT-120 instrument was used to perform transient photo-conductance decay (PCD) measurements and evaluate effective lifetime in samples symmetrically deposited with the ARC. These were used to assess surface passivation by calculating an upper limit to surface recombination velocity as $SRV < W/2(1/\tau_{eff} - 1/\tau_{bulk})$, where τ_{bulk} is taken as that parametrized by Richter in [27]. Both SRV and J_{0s} values were calculated using the same methodology as in [28]. Corona discharge was applied as described in [29] and surface potential charge measurements were conducted on a Kelvin Probe instrument as detailed in [30]. Since water absorption and surface conductivity has been widely suggested to be the principal mechanism for corona charge decay in thin oxide films [31], [32], a hydrophobic hexamethyldisilazane (HMDS) chemical treatment was applied to a subset of specimens prior corona charge deposition. HMDS was applied by subjecting the samples to a 200 °C dehydration anneal for x minutes,

followed by a temperature ramp-down to 120 °C and exposure to HMDS vapor using Ar as carrier gas for x minutes. Optical characterization was performed using both Sentech SE800 PV and JA Woollam M2000 spectroscopic ellipsometers. Reflectance measurements were performed using a customized Tau Science FlashQE system with an integrating sphere and an *X-Y* gantry. The system was configured to raster along the wafer surface measuring the full-spectrum diffuse reflectance at each site creating images of reflectance and current loss due to different mechanisms [33]. Reflectance was measured at 41 wavelengths and were collected at 6,642 sites on the surface of the wafer.

III. Electrical Properties

Metal-insulator-semiconductor test structures consisting of a single TiO_x, single SiO_2, or double SiO_2/ TiO_x coatings were measured using CGV at different frequencies. The resulting capacitance voltage curves are illustrated in Fig. 1. For all three systems, the insulator capacitance was found to depend on the excitation frequency. Higher frequencies led to apparent lower values of insulator capacitance as evidenced by the purple and red traces in Fig. 1. Dielectric leakage and excess series resistance are the common causes for such reduction in C_i. As the frequency is reduced this effect is less pronounced, yet the high frequency condition is less ideal, especially for fast traps at the interface. At frequencies below 1 kHz no noticeable change in the insulator capacitance was observed. Measurements at frequencies of 1 kHz were thus taken as reference to characterize the real insulator capacitance in the accumulation regime. The accuracy of 1 kHz measurements was confirmed for the well-known insulator capacitance of a single SiO_2 layer, which was correctly predicted as shown in Fig. 1.

For the single TiO_x film, lowering of the capacitance for increasing positive gate voltages is observed. This is typical of high leakage currents through the insulator, as detailed in [23] and reported for metal-oxide-semiconductor structures in [34]. The weak depletion regime in CGV measurements of the single TiO_x film was used to infer the C_i. Since the insulator thickness (t) was obtained from optical measurements it was used here to infer the dielectric constant as $K > C_i t/(\varepsilon_0 A)$. For the single layer TiO_x film is found that K_{TiOx} >52. For the double layer, an effective oxide thickness EOT=12.04 nm was calculated thus corresponding to a $K_{TiO_x} = t_{TiO_x} K_{SiO_2}/(EOT - t_{SiO_2})$ >114. The discrepancy in the calculated permittivities could be due to both frequency dispersion, and geometrical effects arising from some of the evaporated aluminum going into pinholes. A true assessment of the TiO_x permittivity is beyond the scope of this work yet it can be concluded that its value is at least 52, which agrees well with previous reports in the literature [35], [36], especially the work of McIntosh *el al.* [37] where a comparable dielectric system was studied.

The inferred flat-band voltages can be used to calculate the concentration of charge in the dielectric coatings when the interface charge is negligible [30], [38], [39], as it has been previously demonstrated for this SiO_2 film [40]. The high leakage in the CGV traces for a single TiO_x film led to an inaccurate calculation of V_{fb}, thus not included here. For the single SiO_2 and double SiO_2/TiO_x coatings, on the other hand, flat-band voltages were calculated and shown in Fig. 1. As deposited SiO_2 was found to have a concentration of +4.17x10^{11} e/cm^2. This is largely due to the dangling bond at a trivalent silicon atom back-bonded to three oxygens, as widely reported in the literature for thermal SiO_2 [23], [41], [42]. Once the APCVD TiO_x coating is deposited the flat-band voltage reduces to -0.06 V thus suggesting that the previously positive concentration of charge in SiO_2 was compensated and surpassed by negative charge. The total charge concentration in the SiO_2/TiO_x double layer was found to be -2.9x10^{11} e/cm^2. This implies the TiO_x deposited in this work is associated with a negative fixed charge concentration of ~7x10^{11} e/cm^2. This is in agreement with the work of McIntosh *el al.* [37], and with work done on atomic layer deposited TiO_x films, where a negative charge was also suggested [43]–[45]. It is of note that

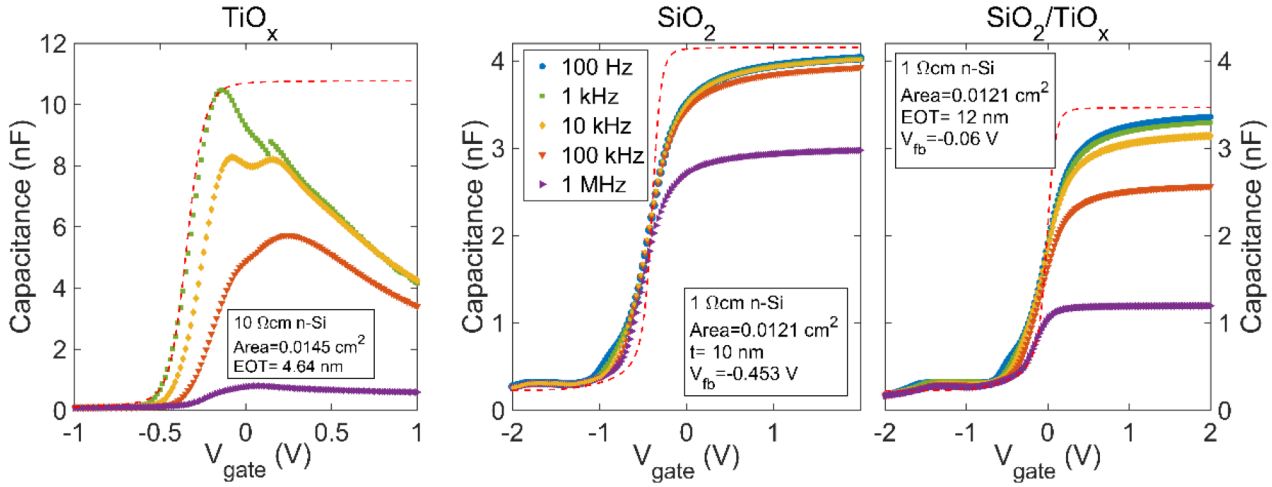

Fig. 1. Capacitance voltage measurements of n-Si/SiO_2, n-Si/TiO_x and n-Si/SiO_2/TiO_x systems. In all cases the theoretical high frequency capacitance-voltage curve shifted by V_{fb} (red dashed line) has been included.

the calculations of Q_f performed here assume that the charge is present at or very near the dielectric-silicon interface. This is a reasonable approximation since Kelvin Probe measurements of these specimens, which are more sensitive to charge towards the surface of the dielectric compared to charge towards the dielectric-silicon interface, showed negligible charge associated with the as-deposited SiO_2/TiO_x films.

The interface trap density (D_{it}) was determined using the Nicollian and Goetzberger [46], [47] conductance method. Measurements of the single TiO_x films were again not possible due to high leakage currents. Fig. 2.a illustrates the resulting D_{it} for three different samples with single SiO_2 or double SiO_2/TiO_x films. These CGV measurements show that the state density at the interface between the SiO_2 and the Si remains largely unchanged after TiO_x deposition. Similar interface state density spectra was also reported in [37] using the high-low capacitance-voltage technique. This was confirmed using photo-conductance decay lifetime measurements of equivalent specimens as illustrated in Fig. 2.b. Here the effective lifetime of 1 Ωcm samples double-sided passivated with single SiO_2 or a double SiO_2/TiO_x coatings is illustrated, before and after extrinsic charge is added via corona. For a starting 100 nm SiO_2 film, APCVD of TiO_x minimally affects the passivation properties as evidenced by the open green and yellow symbols in Fig. 2.b. After positive corona charge deposition the effective lifetimes increased to comparable levels thus suggesting that recombination at the Si-SiO_2 interface remained unaffected by high temperature processing or the presence of the TiO_x layer. For a starting 10 nm SiO_2 film, on the other hand, the TiO_x layer is seen to reduce the effective lifetime to ~40 μs at an injection level $\Delta n=10^{15}$ cm^{-3}. This is attributed to the concentration of negative charge added by the TiO_x deposition, as observed from the flat-band voltage shift in CGV measurements. Negative charge tends to increase the recombination rate (reduce lifetime) at the Si-SiO_2 interface since it increases the concentration of the previously less available holes. This has been previously observed using corona discharge or gate voltage combined with lifetime measurements [32], [48], [49], [40]. Regardless of this decrease in lifetime, once both SiO_2 and SiO_2/TiO_x specimens are positively corona charged (closed blue and red traces), the effective lifetime increases to comparable values supporting the finding that the Si-SiO_2 interface has not been affected by the TiO_x layer.

Sample to sample variations were observed in the maximum effective lifetime samples achieved after corona charging. For 10 nm SiO_2 passivated samples, lifetimes of 1-2 ms were possible, while 100 nm SiO_2 samples showed τ_{eff}~3-4 ms. This is equivalent to a SRV=3.8 cm/s and J_{0s}=8 fA/cm^2, or SRV=1.2 cm/s and J_{0s}=2.2 fA/cm^2, respectively. In comparison to 100 nm SiO_2 specimens, the 10 nm SiO_2 specimens show a best effective lifetime ~2 ms smaller. This effect can be due to (a) a poorer oxide-silicon interface when grown at lower temperatures, and/or (b) the increase in bulk lifetime recently attributed to the annihilation of grown-in defects in FZ silicon that occurs at temperatures exceeding 1000 °C [50], [51], as was the case during growth of the 100 nm SiO_2, but not for the 10 nm. It is to note that samples produced with a 100 nm SiO_2 film only served as comparison in terms of quality and stability of the extrinsic passivation. Thick oxide films are unlikely to be commercial.

Lastly, Fig. 2.b shows the effective lifetime of a sample deposited with an APCVD double layer of 40 nm pc-TiO_x / 70 nm AlO_x at a temperature of 570 °C. In this case effective lifetime was also reduced from the starting 40 μs of a single SiO_2 film, yet after corona discharge deposition the effective lifetime remained the same thus indicating that a substantial diffusion of impurities into the silicon bulk occurred during deposition, most probably due to the higher temperatures required to deposit the AlO_x layer.

The Si-SiO_2 interface was further studied by depositing controlled concentrations of positive and negative corona discharge on the single SiO_2 and double SiO_2/TiO_x specimens while measuring surface potential and effective lifetimes. Fig. 3.a illustrates the dependence of lifetime (at $\Delta n=10^{15}$ cm^{-3}) as the concentration of charge in the dielectrics is progressively increased, for both positive and negative charge polarities. The charge concentration was characterized using the surface

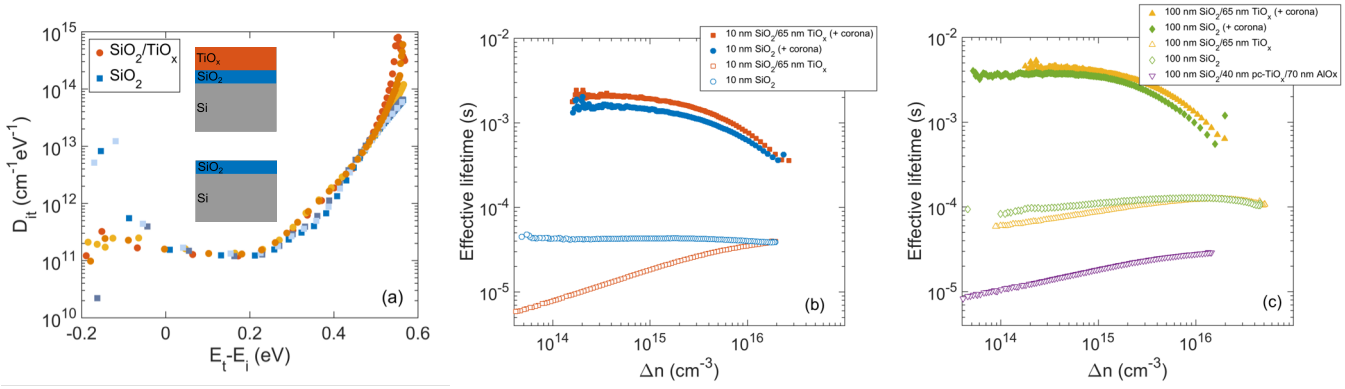

Fig. 2. (a) Interface state density measured using the conductance method in three specimens of a single 10 nm SiO_2 and double 10 nm SiO_2/ 60 nm TiO_x dielectric coatings, (b,c) Effective lifetime measurements of single and double layered passivated 1Ωcm n-type silicon specimens including the contribution of corona discharge to improve field-effect passivation.

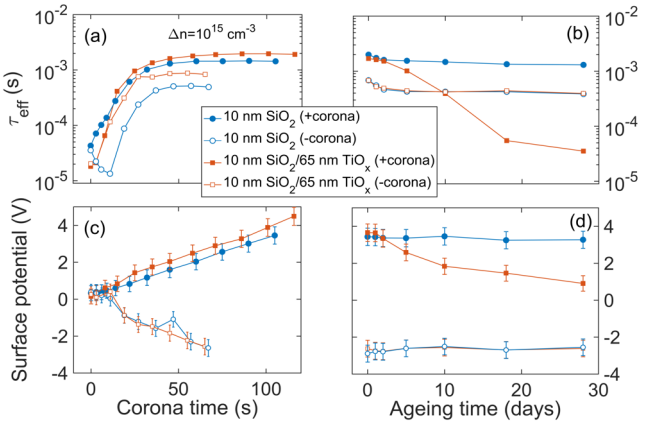

Fig. 3. Effective lifetime as a function of (a) corona charging time and (b) ageing time in laboratory conditions. Surface potential as a function of (c) corona charging time and (d) ageing time in laboratory conditions, for 1Ωcm n-type silicon double-sided passivated with SiO_2 and SiO_2/TiO_x coatings, HMDS treated.

potential and is illustrated in Fig. 3.c. Positive charge directly improves lifetime as the concentration of holes available for recombination is reduced at the Si surface. Negative charge, on the other hand, first increases the concentration of holes thus promoting recombination. This is clearly observed for a single layer SiO_2 specimen since the intrinsic charge concentration was positive, while for a double layered specimen the initial concentration of charge is already negative. Further increase in negative charge in the dielectric then reduces the surface concentration of electrons and increases the effective lifetime of the sample. The maximum effective lifetime achieved for negative charge was 0.5-0.8 ms. This is due to the higher capture velocity for electrons compared to holes at the Si-SiO_2 interface as widely reported in the literature.

From Fig. 3.c it can also be noted that the deposited corona charge migrates directly to the SiO_2-TiO_x interface before it is measured. This can be seen from the equivalent increase in surface potential with time under the corona discharge, since charge was deposited with a constant deposition rate. The dependence of surface potential on charge concentration was reported in [30] as: $V_{KP} = \frac{\Phi_{ms}}{q} + \frac{Q_i x_c}{\varepsilon_0 K_i} + \phi_{scr}$ where x_c is the charge centroid with respect to the silicon surface, Φ_{ms} is the metal to semiconductor work function difference, and ϕ_{scr} is the semiconductor surface potential due to the space charge region. If the deposited corona charge remained at the surface of the double layer film, the quantity x_c/K_i would produce a ~50% larger slope in surface potential as a function of time, in relation to that of the single layer, considering an equivalent dielectric thickness of TiO_x of t_{TiO_x}/K_{TiO_x}= 60 nm / 52. It is therefore concluded that the equivalent slopes observed in the surface potential versus charging time in Fig. 3.c are only possible if the charge is located at the surface of the SiO_2 layer in both cases.

Four additional specimens were HMDS treated and charged in a single step by the optimal amount of time found when doing the charging process in steps (Fig. 3.a and c). These were then kept in laboratory conditions and measured periodically as shown in Fig. 3.b and d. Only for the positively charged SiO_2/TiO_x film was a rapid decay in effective lifetime observed, relating to a decrease in the field effect passivation provided by the corona charge. It is hypothesized that such charge leakage is related to the preferable electron conduction in TiO_x films as reported by Yang in [52], [53], yet no further investigations have been conducted here. The decay of positive charge from the DLARC can be addressed as suggested by other reports where extrinsic field effect passivation is provided using potassium charged ions in the dielectric coatings [21], [54]. Corona charging of these dielectric films is used here only as proof of principle, thus providing a limit to the surface passivation attainable using these dielectrics.

IV. Optical Properties

Use Spectroscopic ellipsometry measurements were performed on the a-TiO_x films deposited on polished Cz Si specimens. These showed equivalent n and k values to those found in prior work using the same process parameters for the APCVD process [22]. These were later used as the input parameter to simulate the reflectance from wafers textured with up-right random pyramids, and deposited with a-TiO_x. The reflectance from such specimens was experimentally measured as detailed in Section II, and was compared to the reflectance of textured wafers featuring a SiN_x ARC. The measured and simulated reflectance spectra are shown in Fig. 4.a and b, for the nitride and titania films respectively. Front surface reflectance and parasitic absorption within the ARC were simulated using OPAL2 [55]. The error bars indicate the standard deviation of the reflectance taken from all 6,642 measurements on the wafer surface. The deviation between the measured and simulated spectra at wavelengths above 1 µm is due to light internally reflected off the rear wafer surface back to the top of the wafer (i.e., escape reflectance). Here it is clear that the optical performance of the deposited a-TiO_x films is, at least, comparable to that of standard SiN_x film, when the specimens are not encapsulated.

The reflection values measured at each point were converted to current losses using the approach described in [33]. A full-area spatial map of the resulting current lost due to reflection (J_R) for the a-TiO_x ARC on an industrial-scale (156 mm x 156 mm) textured wafer is shown in Fig. 4.c. Here it is evident that the deposition process is relatively uniform over the whole surface of the wafer, with some thickness variation occurring near the right edge of the wafer resulting in slightly higher reflectance. With further optimizations, the uniformity of this process can be improved and made compatible with the demands of high-volume manufacturers.

It is also noted that the film thickness obtained on polished samples was ≈64 nm. However, optical simulations performed with OPAL 2 [55], matched to the reflectance data, reveal a slightly thinner film (≈59 nm) for the textured wafers. This has been empirically observed and can be explained by the fixed flux of precursor species being transported to a larger surface

area for the textured samples. In addition, the growth reaction is mass transport limited and thus a thinner film might be expected in textured specimens.

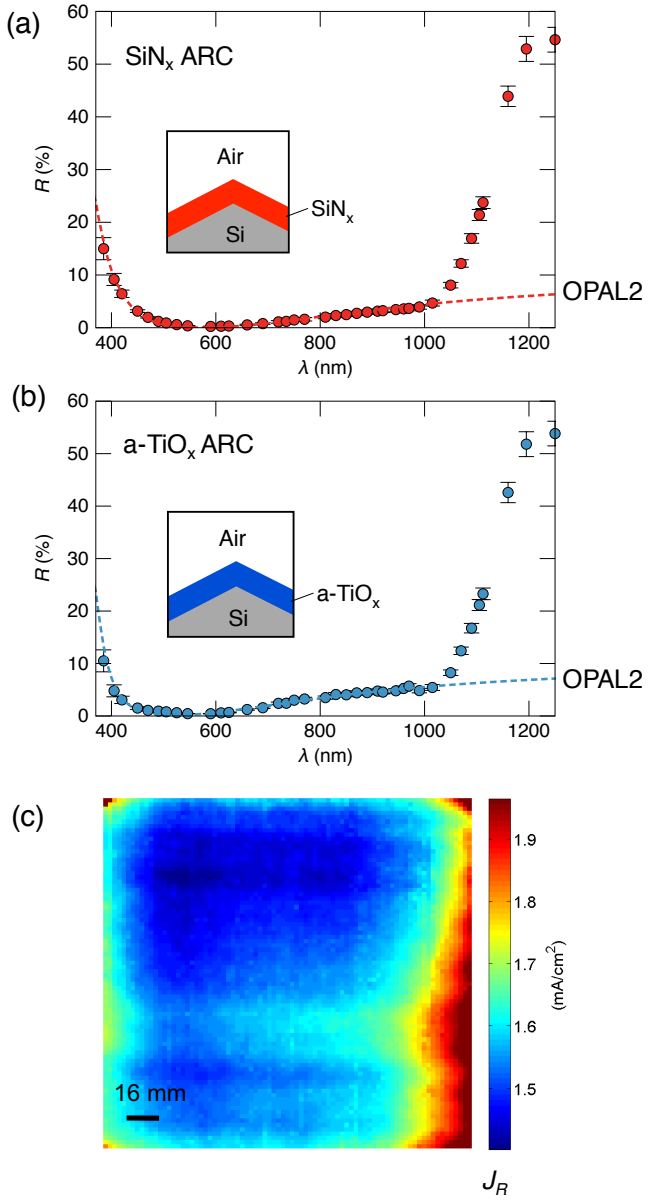

Fig. 4. Measured (circles) and simulated (dashed lines) front surface reflectance spectra for textured wafers (i.e., random upright pyramids) featuring: (a) a SiN_x ARC; and (b) an a-TiO_x ARC. (c) A full area spatial map of current loss, J_R, due to surface reflectance for a industrial-scale (156 mm x 156 mm) textured wafer coated with a-TiO_x.

In addition to the samples fabricated and measured, simulations were also carried out on potential ARC structures based on the a-TiO_x and pc-TiO_x produced here. These structures are shown in Fig. 5.a. They include an a-TiO_x with an optimized film thickness (69 nm); a 10 nm SiO_2 passivation layer followed by a 55 nm a-TiO_x film; and a 10 nm SiO_2 passivation layer followed by a 45 nm pc-TiO_x film and a 93 nm AlO_x film. The thicknesses have been chosen to maximize absorption of sunlight into the underlying silicon. The simulated front surface reflectance spectra for these different ARC structures is given for unencapsulated cells (i.e., air as the incident medium with n = 1) in Fig. 5.b and for encapsulated cells (i.e., EVA as the incident medium with $n \approx 1.5$) in Fig. 5 (c). In the encapsulated case reference is only made to optimized structures since no experimental data is available in presence of an EVA film. These were simulated as the optimal for encapsulated absorption. These simulated reflectance spectra were used to calculate the resulting losses J_R and the parasitic absorption within the ARC film(s) (J_A). The reflection and absorption values are converted to current losses using the methodology described in [55]. These are shown in Fig. 6, for both unencapsulated and encapsulated cells.

For the unencapsulated case, the a-TiO_x ARC featuring a 10 nm SiO_2 passivation layer and the SiN_x ARC have a nearly identical combined current loss (i.e., $J_R + J_A$) of ≈1.5 mA/cm^2. When encapsulated though, the SiO_2/a-TiO_x ARC has a combined current loss of only 0.78 mA/cm^2, compared to 0.93 mA/cm^2 for the encapsulated SiN_x ARC. The double layer pc-TiO_x / AlO_x ARC featuring a 10 nm SiO_2 passivation layer has a significantly lower combined current loss than both the SiO_2/a-TiO_x and SiN_x ARCs when unencapsulated, but is only marginally lower than SiO_2/a-TiO_x at 0.65 mA/cm^2 when encapsulated. Overall, these simulations indicate that a gain in optical performance can be achieved from the titania films studied here. When thickness is optimized, a SiO_2/TiO_x double layer ARC can produce ≈0.2 mA/cm^2 less optical losses on the surface of the cell, compared to a reference SiN_x film. A triple layer SiO_2/pc-TiO_x/AlO_x ARC can perform even better reducing losses in ≈0.3 mA/cm^2. Given the multiple advantages of APCVD in comparison to PECVD, these titania films are seen as potential replacements for improved antireflection in silicon solar cells. It is noted, however, that hydrogenation is a key aspect in which PECVD nitrides outperform other dielectric systems. New processing for extrinsic hydrogenation has been recently proposed to address this shortfall [56], [57]. The use of such techniques could bring independent improvements in chemical passivation of the cell's bulk and interfaces.

V. Conclusion

The present work has demonstrated that effective passivation and anti-reflection can be achieved using a film stack consisting of a 10 nm silicon dioxide (SiO_2) film followed by ~65 nm amorphous titanium oxide (a-TiO_x). This film is industrially relevant since fast processes to produce thin SiO_2 layers are currently available, while ultra-high throughput APCVD is used to deposit a-TiOx. The passivation properties of such layers were demonstrated on flat 1 Ωcm Si specimens producing effective lifetimes as high as 1-2 ms, equivalent to a SRV as low as 3.8 cm/s, or J_{0s}<8 fA/cm^2. Optically, this layer showed equivalent performance to SiN_x for unencapsulated cells, and ≈0.2 mA·cm^{-2} better performance for encapsulated cells. To the authors' knowledge, no dielectric stack featuring TiO_x where effective passivation and optical properties are effectively achieved has

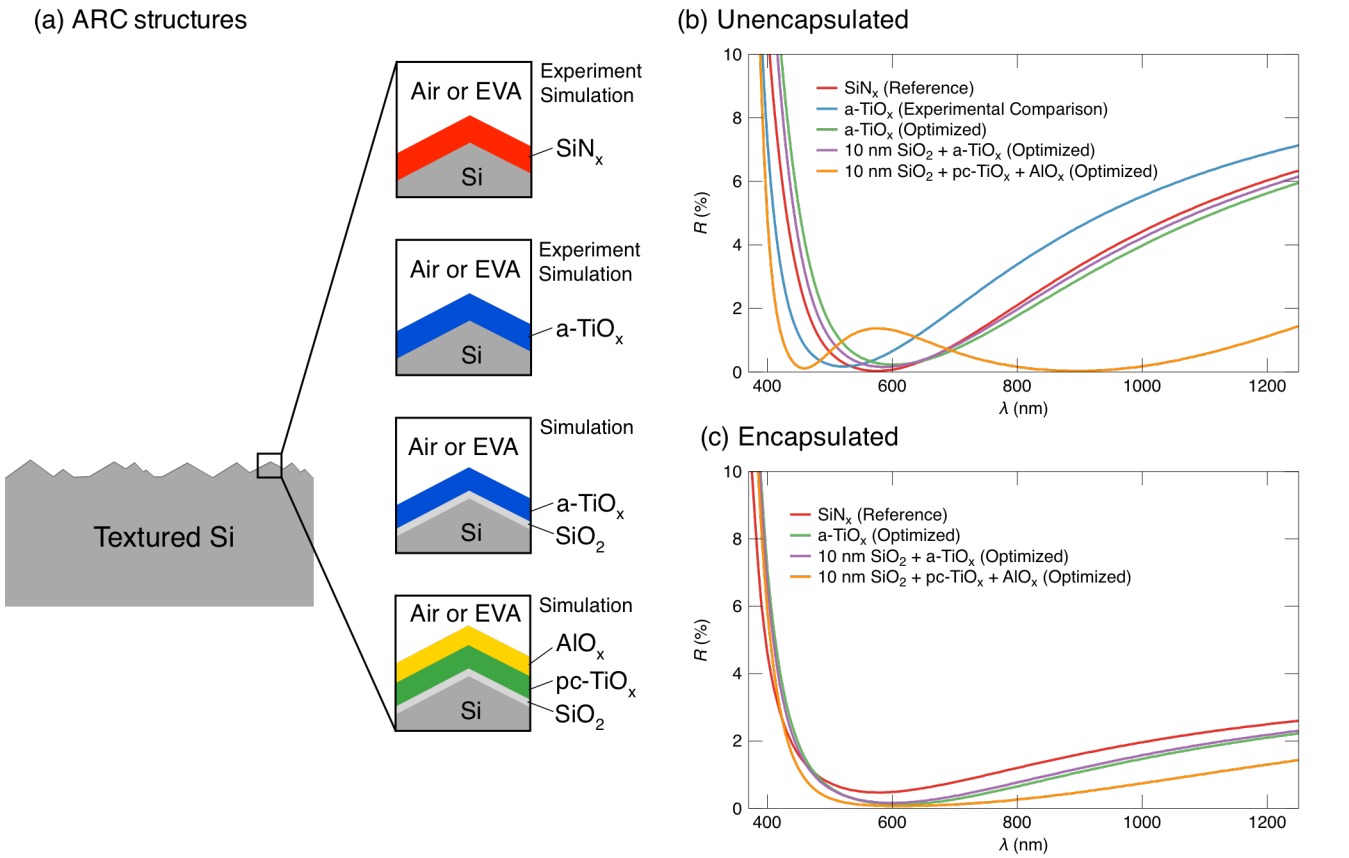

Fig. 5. (a) Illustration of the ARC structures investigated in this work. Simulated front surface reflectance spectra for (b) unencapsulated cells and (c) encapsulated cells, where unencapsulated cells feature air as the incident medium (n = 1) and encapsulated cells feature EVA as the incident medium (n ≈ 1.5).

been yet reported. Furthermore, optical simulations indicated that 0.3 mA·cm^{-2} gain in optical performance is possible when a double-layer ARC featuring a polycrystalline TiO_x (pc-TiO_x) film followed by an aluminum oxide (AlO_x) is used. However, when such layers were investigated experimentally the effective lifetime of the samples was < 100 μs, most likely due to contamination during APCVD deposition at the high temperatures used.

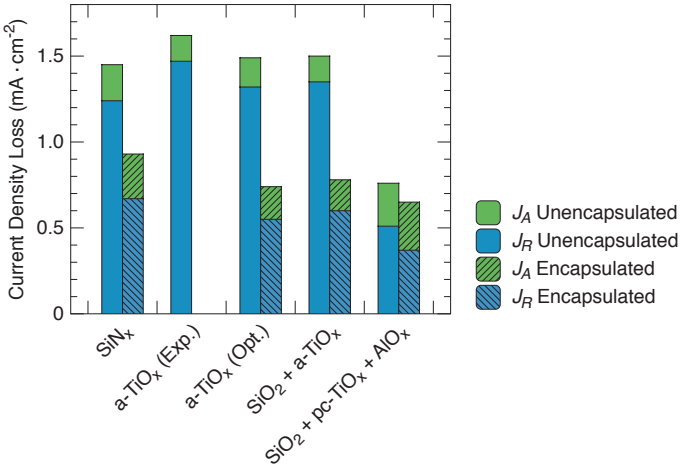

Fig. 6. Resulting current density losses, including current lost due to reflection (J_R) and parasitic absorption within the ARC film(s) (J_A). Results are given for unencapsulated and encapsulated cells.

ACKNOWLEDGMENT

RS Bonilla is the recipient of an EPSRC (UK) Postdoctoral Research Fellowship, EP/M022196/1. PR Wilshaw acknowledges the support from EPSRC grant EP/M024911/1. All authors are thankful to Christian Reichel for oxide preparation at Fraunhofer ISE, and to Heiko Zunft for help with APCVD at SCHMID. Data published in this article can be downloaded from http://ora.ox.ac.uk

REFERENCES

[1] E. Kern, K. ; Tracy, "Titanium dioxide antireflection coating for silicon solar cells by spray deposition," *RCA Rev*, vol. 41, 1980.

[2] M. Murozono, S. Kitamura, T. Ohmura, K. Kusao, and Y. Umeo, "Titanium Dioxide Antireflective Coating for Silicon Solar Cells by Spinning Technique," *Japanese Journal of Applied Physics*, vol. 21, no. S2, p. 137, Jan. 1982.

[3] D. C. Wong and A. Waugh, "Cost Impacts of Anti-Reflection Coatings on Silicon Solar Cells," *MRS Proceedings*, vol. 426, p. 503, Jan. 1996.

[4] J. Szlufcik, J. Majewski, A. Buczkowski, J. Radojewski, L. Jędral, and E. B. Radojewska, "Screen-printed titanium dioxide anti-reflection coating for silicon solar cells," *Solar Energy Materials*, vol. 18, no. 5, pp. 241–252, 1989.

[5] B. S. Richards, "Single-material TiO2 double-layer antireflection coatings," *Solar Energy Materials and Solar Cells*, vol. 79, no. 3, pp. 369–390, 2003.

[6] T. Watanabe *et al.*, "Photocatalytic activity and photoinduced hydrophilicity of titanium dioxide coated glass," *Thin Solid Films*, vol. 351, no. 1, pp. 260–263, 1999.

[7] S. A. O'Neill, I. P. Parkin, R. J. H. Clark, A. Mills, and N. Elliott, "Atmospheric pressure chemical vapour deposition of titanium dioxide coatings on glass," *Journal of Materials Chemistry*, vol. 13, no. 1, pp. 56–60, Dec. 2003.

[8] B. S. Richards, "Comparison of TiO2 and other dielectric coatings for buried-contact solar cells: a review," *Progress in Photovoltaics: Research and Applications*, vol. 12, no. 4, pp. 253–281, Jun. 2004.

[9] S. Duttagupta, F. Lin, M. Wilson, M. B. Boreland, B. Hoex, and A. G. Aberle, "Extremely low surface recombination velocities on low-resistivity n -type and p -type crystalline silicon using dynamically deposited remote plasma silicon nitride films," *Progress in Photovoltaics: Research and Applications*, vol. 22, no. 6, pp. 641–647, Jun. 2014.

[10] J. Schmidt and A. G. Aberle, "Carrier recombination at silicon-silicon nitride interfaces fabricated by plasma-enhanced chemical vapor deposition," *Journal of Applied Physics*, vol. 85, no. 7, pp. 3626–3633, 1999.

[11] Y. Ren, K. J. Weber, N. M. Nursam, and D. Wang, "Effect of deposition conditions and thermal annealing on the charge trapping properties of SiN[sub x] films," *Applied Physics Letters*, vol. 97, no. 20, p. 202907, Nov. 2010.

[12] J. Schmidt, M. Kerr, and A. Cuevas, "Surface passivation of silicon solar cells using plasma-enhanced chemical-vapour-deposited SiN films and thin thermal SiO 2 /plasma SiN stacks," *Semiconductor Science and Technology*, vol. 16, no. 3, pp. 164–170, Mar. 2001.

[13] J. Schmidt and M. Kerr, "Highest-quality surface passivation of low-resistivity p-type silicon using stoichiometric PECVD silicon nitride," *Solar Energy Materials and Solar Cells*, vol. 65, no. 1, pp. 585–591, 2001.

[14] B. Hoex, S. B. S. Heil, E. Langereis, M. C. M. van de Sanden, and W. M. M. Kessels, "Ultralow surface recombination of c-Si substrates passivated by plasma-assisted atomic layer deposited Al2O3," *Applied Physics Letters*, vol. 89, no. 4, p. 42112, Jul. 2006.

[15] J. Y. Lee, J. Dicker, S. Rein, and S. W. Glunz, "Investigation of various surface passivation layers using oxide/nitride stacks of silicon solar cells," in *Photovoltaic Energy Conversion, 2003. Proceedings of 3rd World Conference*, 2003, vol. 2, p. 1069–1072 Vol.2.

[16] M. Hofmann *et al.*, "Recent developments in rear-surface passivation at Fraunhofer ISE," *Solar Energy Materials and Solar Cells*, vol. 93, no. 6–7, pp. 1074–1078, 2009.

[17] M. Lamers *et al.*, "The interface of a-SiNx:H and Si: Linking the nano-scale structure to passivation quality," *Solar Energy Materials and Solar Cells*, 2013.

[18] A. F. Thomson and K. R. McIntosh, "Light-enhanced surface passivation of TiO_2 -coated silicon," *Progress in Photovoltaics: Research and Applications*, vol. 20, no. 3, pp. 343–349, May 2012.

[19] M. J. Kerr, J. Schmidt, A. Cuevas, and J. H. Bultman, "Surface recombination velocity of phosphorus-diffused silicon solar cell emitters passivated with plasma enhanced chemical vapor deposited silicon nitride and thermal silicon oxide," *Journal of Applied Physics*, vol. 89, no. 7, pp. 3821–3826, 2001.

[20] L. E. Black, T. Allen, K. R. McIntosh, and A. Cuévas, "Improved Silicon Surface Passivation of APCVD Al2O3 by Rapid Thermal Annealing," *Energy Procedia*, vol. 92, pp. 317–325, 2016.

[21] R. S. Bonilla and P. R. Wilshaw, "A technique for field effect surface passivation for silicon solar cells," *Applied Physics Letters*, vol. 104, no. 23, p. 232903, Jun. 2014.

[22] K. O. Davis, K. Jiang, D. Habermann, and W. V. Schoenfeld, "Tailoring the Optical Properties of APCVD Titanium Oxide Films for All-Oxide Multilayer Antireflection Coatings," *IEEE Journal of Photovoltaics*, vol. 5, no. 5, pp. 1265–1270, Sep. 2015.

[23] E. H. Nicollian and J. R. Brews, *MOS (Metal Oxide Semiconductor) — Physics and Technology*. Wiley, New York, 1982.

[24] M. J. McNutt and C. T. Sah, "Determination of the MOS oxide capacitance," *Journal of Applied Physics*, vol. 46, no. 9, p. 3909, 1975.

[25] S. V. Walstra and C.-T. Sah, "EXTENSION OF THE McNUTT-SAH METHOD FOR MEASURING THIN OXIDE THICKNESSES OF MOS DEVICES," *Solid-State Electronics*, vol. 42, no. 4, pp. 671–673, 1998.

[26] S. M. S. Sze, N. Kwok Kwok, and K. K. Ng, *Physics of Semiconductor Devices*, Third Edit. Hoboken, New Jersey: John Wiley and Sons, Inc, 2007.

[27] A. Richter, S. W. Glunz, F. Werner, J. Schmidt, and A. Cuevas, "Improved quantitative description of Auger recombination in crystalline silicon," *Physical Review B*, vol. 86, no. 16, p. 165202, Oct. 2012.

[28] R. S. Bonilla, B. Hoex, P. Hamer, and P. R. Wilshaw, "Dielectric surface passivation for silicon solar cells: A review," *physica status solidi (a)*, vol. 214, no. 7, p. 1700293, 2017.

[29] R. S. Bonilla, F. Woodcock, and P. R. Wilshaw, "Very low surface recombination velocity in n-type c-Si using extrinsic field effect passivation," *Journal of Applied Physics*, vol. 116, no. 5, p. 54102, 2014.

[30] R. S. Bonilla, N. Jennison, D. Clayton-Warwick, K. A. Collett, L. Rands, and P. R. Wilshaw, "Corona charge in SiO2: kinetics and surface passivation for high efficiency silicon solar cells," *Energy Procedia*, vol. 92, pp. 326–335, Aug. 2016.

[31] W. Olthuis and P. Bergveld, "On the charge storage and decay mechanism in silicon dioxide electrets," *IEEE Transactions on Electrical Insulation*, vol. 27,

no. 4, pp. 691–697, 1992.
[32] R. S. Bonilla, C. Reichel, M. Hermle, P. Hamer, and P. R. Wilshaw, "Long term stability of c-Si surface passivation using corona charged SiO2," *Applied Surface Science*, vol. 412, pp. 657–667, 2017.
[33] E. J. Schneller, K. Ogutman, S. Guo, W. V. Schoenfeld, and K. O. Davis, "Crystalline Silicon Device Loss Analysis Through Spatially Resolved Quantum Efficiency Measurements," *IEEE Journal of Photovoltaics*, vol. 7, no. 4, pp. 957–965, Jul. 2017.
[34] D. P. Norton, "Capacitance–voltage measurements on ultrathin gate dielectrics," *Solid-State Electronics*, vol. 47, no. 5, pp. 801–805, 2003.
[35] M.-K. Lee, H.-C. Lee, and C.-M. Hsu, "High dielectric constant titanium oxide grown on amorphous silicon by metal-organic chemical vapour deposition," *Semiconductor Science and Technology*, vol. 21, no. 5, pp. 604–607, May 2006.
[36] M.-K. Lee, J.-J. Huang, and T.-S. Wu, "Electrical characteristics improvement of oxygen-annealed MOCVD-TiO $_2$ films," *Semiconductor Science and Technology*, vol. 20, no. 6, pp. 519–523, Jun. 2005.
[37] K. R. McIntosh, S. C. Baker-Finch, N. E. Grant, A. F. Thomson, S. Singh, and I. D. Baikie, "Charge Density in Atmospheric Pressure Chemical Vapor Deposition TiO2 on SiO2-Passivated Silicon," *Journal of The Electrochemical Society*, vol. 156, no. 11, p. G190, Nov. 2009.
[38] E. H. Snow, A. S. Grove, B. E. Deal, and C. T. Sah, "Ion Transport Phenomena in Insulating Films," *Journal of Applied Physics*, vol. 36, no. 5, pp. 1664–1673, 1965.
[39] T. C. Kho, S. C. Baker-Finch, and K. R. McIntosh, "The study of thermal silicon dioxide electrets formed by corona discharge and rapid-thermal annealing," *Journal of Applied Physics*, vol. 109, p. 53108, 2011.
[40] R. S. Bonilla and P. R. Wilshaw, "On the c-Si/SiO2 interface recombination parameters from photo-conductance decay measurements," *Journal of Applied Physics*, vol. 121, no. 13, p. 135301, Apr. 2017.
[41] W. Füssel, M. Schmidt, H. Angermann, G. Mende, and H. Flietner, "Defects at the Si/SiO2 interface: Their nature and behaviour in technological processes and stress," *Nuclear Instruments and Methods in Physics Research, Section A: Accelerators, Spectrometers, Detectors and Associated Equipment*, vol. 377, no. 2–3, pp. 177–183, Aug. 1996.
[42] A. G. Aberle, *Crystalline Silicon Solar Cells: advanced surface passivation and analysis*. Sydney, Australia: UNSW, 2009.
[43] J. Cui *et al.*, "Titanium oxide: A re-emerging optical and passivating material for silicon solar cells," *Solar Energy Materials and Solar Cells*, vol. 158, pp. 115–121, Dec. 2016.
[44] B. Liao, B. Hoex, K. D. Shetty, P. K. Basu, and C. S. Bhatia, "Passivation of Boron-Doped Industrial Silicon Emitters by Thermal Atomic Layer Deposited Titanium Oxide," *IEEE Journal of Photovoltaics*, vol. 5, no. 4, pp. 1062–1066, Jul. 2015.
[45] B. Liao *et al.*, "Excellent *c* -Si surface passivation by thermal atomic layer deposited aluminum oxide after industrial firing activation," *Journal of Physics D: Applied Physics*, vol. 46, no. 38, p. 385102, Sep. 2013.
[46] E. H. Nicollian and A. Goetzberger, "MOS Conductance Technique for Measuring Surface State Parameters," *Applied Physics Letters*, vol. 7, no. 8, p. 216, Nov. 1965.
[47] E. H. Nicollian and A. Goetzberger, "The Si-SiO2 Interface — Electrical Properties as Determined by the Metal-Insulator-Silicon Conductance Technique," *Bell System Technical Journal*, vol. 46, no. 6, pp. 1055–1133, Jul. 1967.
[48] S. W. Glunz, D. Biro, S. Rein, and W. Warta, "Field-effect passivation of the SiO2Si interface," *Journal of Applied Physics*, vol. 86, no. 1, pp. 683–691, Jul. 1999.
[49] H. Haug, S. Olibet, Ø. Nordseth, and E. Stensrud Marstein, "Modulating the field-effect passivation at the SiO2/c-Si interface: Analysis and verification of the photoluminescence imaging under applied bias method," *Journal of Applied Physics*, vol. 114, no. 17, p. 174502, Nov. 2013.
[50] N. E. Grant, V. P. Markevich, J. Mullins, A. R. Peaker, F. Rougieux, and D. Macdonald, "Thermal activation and deactivation of grown-in defects limiting the lifetime of float-zone silicon," *physica status solidi (RRL) - Rapid Research Letters*, vol. 10, no. 6, pp. 443–447, Jun. 2016.
[51] N. E. Grant, F. E. Rougieux, D. Macdonald, J. Bullock, and Y. Wan, "Grown-in defects limiting the bulk lifetime of p-type float-zone silicon wafers," *Journal of Applied Physics*, vol. 117, no. 5, p. 55711, Feb. 2015.
[52] X. Yang, Q. Bi, H. Ali, K. Davis, W. V. Schoenfeld, and K. Weber, "High-Performance TiO2-Based Electron-Selective Contacts for Crystalline Silicon Solar Cells," *Advanced Materials*, vol. 28, no. 28, pp. 5891–5897, Jul. 2016.
[53] X. Yang, P. Zheng, Q. Bi, and K. Weber, "Silicon heterojunction solar cells with electron selective TiOx contact," *Solar Energy Materials and Solar Cells*, vol. 150, pp. 32–38, 2016.
[54] R. S. Bonilla, K. Collett, L. Rands, G. Martins, R. Lobo, and P. R. Wilshaw, "Stable, Extrinsic, Field Effect Passivation for Back Contact Silicon Solar Cells," *Solid State Phenomena*, vol. 242, pp. 67–72, Oct. 2015.
[55] K. R. McIntosh and S. C. Baker-Finch, "OPAL 2: Rapid optical simulation of silicon solar cells," in *2012 38th IEEE Photovoltaic Specialists Conference*, 2012, pp. 000265–000271.
[56] P. Hamer, G. Bourret-Sicotte, G. Martins, A. Wenham, R. S. Bonilla, and P. Wilshaw, "A Novel Source of Atomic Hydrogen for Passivation of Silicon Solar Cells," *physica status solidi RRL*, vol. 11, no. 5, p. 1600448, 2017.
[57] G. Bourret-Sicotte *et al.*, "Shielded hydrogen passivation − A potential in-line passivation process," *physica status solidi (a)*, vol. 214, no. 7, p. 1700383,

Jul. 2017.